

Hydrodynamic Simulation of Centrifugal Pumps under One-Phase and Two-Phase Flow Conditions – Effect of Blade Numbers

Amin Habibi Sarbanani

Department of Mechanical Engineering, Kerman Branch, Islamic Azad University,
Kerman, Iran.

Abstract— Centrifugal pumps are most commonly used in different fields like industries, agriculture and domestic applications. CFD tool is used for simulation of the flow field characteristics inside the turbo machinery. This numerical method makes it possible to visualize the flow condition inside the centrifugal pump. In the present work, simulation was steady and moving reference frame was used to consider the impeller-volute interaction. One-phase and two-phase solid-liquid flow in a centrifugal pump with the different blade number of impeller has been modeled using the Eulerian-Eulerian approach with mixture multiphase model and granular options in a commercial CFD code. Standard $k-\varepsilon$ turbulence mode has been used for modeling turbulence. Second order upwind scheme is considered for the discretization of momentum, k and ε equations, while SIMPLE algorithm has been applied for dealing with pressure-velocity coupling. Results are validated with comparing computed flow rate with analytical solution. From the obtained numerical results, a detailed situation of the flow in the pump is visualized, including the pressure and velocity distributions. Finally, the head-capacity in one-phase and two-phase flows with different blade numbers are compared to each other. It was observed that CFD simulation results give good prediction of characteristics of centrifugal pump and may help to reduce the required experimental work for the study of centrifugal pump characteristics.

Keywords- Centrifugal pump, CFD simulation, tow-phase fluid, static pressure, pump head

I. INTRODUCTION

Pump designers are continually challenged to provide machines that operate more efficiently, quietly, and reliably at lower cost. Key to design a hydraulic turbomachine is a detailed understanding of the internal flow within its stationary and rotating passages and therefore the calculability of its performance during design and off-design conditions. With the aid of the Computational Fluid Dynamics (CFD) approach, the complex internal flows in water pump centrifugal impellers, which are not fully understood yet, can be well predicted and therefore establishing the CFD as a key tool for pump designers. The use of CFD tools in turbomachinery industry is quite common today since many tasks can numerically be solved much faster and cheaper than by means of experiments. Commercial software Fluent, CFX-Tascflow, StarCD and Fine/Turbo, is increasingly using to study pump design and off-design performance [1]. Asuaje et al. [2] performed a 3D-CFD simulation of impeller and volute of a centrifugal pump using CFX code with a specific speed of 32. In this simulation, structured grid was used in the impeller and unstructured grid in the volute, while $k-\varepsilon$, $k-\omega$ and SST turbulent models were used. They found velocity and pressure fields for different flow rates and radial thrust on the pump shaft. Mentzos et al. [3] carried out a numerical simulation of the internal flow in a backward curve vaned centrifugal pump. The MRF approach used to take into account the impeller-volute interaction. However, its use was recommended for basic understanding of the flow at various operating points. The transient analysis was suggested as a real tool for understanding of the interaction between impeller and spiral casing. Mentzos et al. [1] simulated the flow through the impeller of centrifugal pump using finite-volume method along with a structured grid system for the solution of the discretized governing equations. The CFD technique was applied to predict the flow patterns, pressure distribution and head-capacity curve. It was reported that, although the grid size was not adequate to investigate the local boundary layer variables, global ones were well captured. The proposed approach was advocated for the basic understanding of the flow at various operating points. Baoling et al. [4] investigated the effect of number of splitting blades for long, mid and short blades using a one-equation turbulent model. Their computations were performed using commercial Fine/Turbo 6.2 at a specific speed of 18. Their results show that the bulk flow in the impeller has an important influence on the pump performance. Bacharoudis et al. [5] analyzed the performance of pump by varying the outlet blade angles by keeping the same outlet diameter. The numerical simulation of 3-D, incompressible Navier-Stokes equations was carried out with a commercial CFD finite-volume code. At nominal capacity, when the outlet blade angle was increased from 20° to 50° , the head was increased by more than 6% but the hydraulic efficiency was reduced by 4.5%. However, at high flow rates, the increase of the outlet blade angle caused a significant improvement of the hydraulic efficiency. Caridad et al. [6] carried out numerical analysis in a centrifugal pump impeller of submersible pump conveying an air–water mixture, which was similar to cavitating flow. A sensibility analysis with regard to the gas-void fraction and the bubble diameter was performed. The

variations in impeller head and relative flow angle at the outlet were presented as a function of liquid flow rate and phase distribution within the impeller. It was found that, larger bubble diameter lead to larger head experimented by the impeller. The numerical results and diffuser losses showed excellent agreement with the experimental results. Pagalthivarthi et al. [7] simulated dense slurry flow through centrifugal pump casing using the Eulerian multiphase model in Fluent 6.1. First order upwind scheme was considered for the discretization of momentum, k and ϵ terms and a mixture property based k - ϵ turbulence model was used for modeling turbulence. The effects of pump flow rate, tongue curvature, casing width, inlet concentration of the particles was considered on wall stress distribution and velocities along the wall. Analysis concluded that solid concentration and solid wall shear stress increase monotonically from the upstream of the tongue to the downstream of the belly region. Anagnostopoulos, [8] simulated 3D turbulent flow in a radial pump impeller for a constant rotational speed of 1500 rpm based on the solution of the RANS equations. The flow equations were discretized using the control volume approach, and the standard k - ϵ model was adopted for the turbulence closure. The computations for the steady flow field in a particular impeller were presented. The characteristic performance curves for the entire load range of the impeller were constructed, and their pattern was found reasonable and in agreement with theory. None of the previous works includes study of 3D modeling within a full domain considering interaction between rotor and stator of a high centrifugal pump using various turbulence models. In this paper, the centrifugal pump flow simulation was done with handling both water as a single phase fluid and solid-liquid two-phase one. For these numerical simulations, the SIMPLE algorithm is used for solving governing equations of incompressible viscous/turbulent flows through the pump. The k - ϵ turbulence model is adopted to describe the turbulent flow process. These simulations have been made with using the Multiple Reference Frames (MRF) technique to take into account the impeller-volute interaction. For solid-liquid two-phase fluid mixture, a suitable model with granular option are developed.

II. GOVERNING EQUATIONS

A. One-Phase Fluid

Since, the fluid surrounding the impeller rotates around the axis of the pump, the fundamental equations of fluid dynamics must be organized in two reference frames, stationary and rotating reference frames. To accomplish this, the Multiple Reference Frame (MRF) model has been used here. The basic idea of the model is to simplify the flow inside the pump into an instantaneous flow at one position, to solve unsteady-state problem with steady-state method. In this approach, the governing equations are set in a rotating reference frame, and Coriolis and centrifugal forces are added as source terms.

Continuity and momentum equations for an incompressible flow are as the following:

$$\nabla \cdot \mathbf{u} = 0 \quad (1)$$

$$\nabla \cdot (\rho \mathbf{u} \mathbf{u}) = -\nabla p + \nabla \tau + \mathbf{s} \quad (2)$$

In the above equations, \mathbf{u} is the relative velocity of fluid, τ is the stress tensor and \mathbf{s} is the source term, which consists of Coriolis and centrifugal forces:

$$\mathbf{s} = -2\rho \boldsymbol{\Omega} \times \mathbf{u} - \rho \boldsymbol{\Omega} \times (\boldsymbol{\Omega} \times \mathbf{r}) \quad (3)$$

Here $\boldsymbol{\Omega}$ is rotational speed and \mathbf{r} position vector.

B. Two-Phase Fluid

The calculation of the solid-liquid two-phase flow field adopts the mixture multiphase flow model, and standard k - ϵ turbulence model.

The continuity equation of the mixture model can be expressed as:

$$\frac{\partial}{\partial t}(\rho_m) + \nabla \cdot (\rho_m \vec{v}_m) = 0 \quad (4)$$

where \vec{v}_m is the mass-averaged velocity:

$$\vec{v}_m = \frac{\sum_{k=1}^n \alpha_k \rho_k \vec{v}_k}{\rho_m} \quad (5)$$

and ρ_m is the mixture density:

$$\rho_m = \sum_{k=1}^n \alpha_k \rho_k \quad (6)$$

α_k is the volume fraction of phase k .

The momentum equation for the mixture can be obtained by summing the individual momentum equations for all phases. It can be expressed as:

$$\frac{\partial}{\partial t} (\rho_m \vec{v}_m) + \nabla \cdot (\rho_m \vec{v}_m \vec{v}_m) = -\nabla p + \nabla \cdot [\mu_m (\nabla \vec{v}_m + \nabla \vec{v}_m^T)] + \rho_m \vec{g} + \vec{F} + \nabla \cdot \left(\sum_{k=1}^n \alpha_k \rho_k \vec{v}_{dr,k} \vec{v}_{dr,k} \right) \quad (7)$$

where n is the number of phases, \vec{F} is a body force, and μ_m is the viscosity of the mixture:

$$\mu_m = \sum_{k=1}^n \alpha_k \mu_k \quad (8)$$

$\vec{v}_{dr,k}$ is the drift velocity for secondary phase k :

$$\vec{v}_{dr,k} = \vec{v}_k - \vec{v}_m \quad (9)$$

Volume fraction equation:

$$\frac{\partial}{\partial t} (\alpha_p \rho_p) + \nabla \cdot (\alpha_p \rho_p \vec{v}_m) = -\nabla \cdot (\alpha_p \rho_p \vec{v}_{dr,p}) \quad (10)$$

III. DESCRIPTION OF THE MODEL

The geometry is complex and asymmetric due to the blade and volute shape. It is the first thing using CAD software to define the geometry of the pump impeller. Then the Gambit as the preprocessing software is employed to develop the geometry and to get the mesh. The based model contains six blades impeller spaced 60° between them with 3 mm of thickness. A triangular mesh was selected for meshing the flow domain. The impeller has an outlet diameter of 184 mm and inlet diameter of 62 mm, while the eye diameter is 46mm. The model is divided into three boundary zone types (inlet, impeller and volute). The mesh file contains the coordinates of all the nodes, connectivity information that tells how the nodes are connected to one another to form faces and cells, and zone types and number of all the faces. The grid file does not contain any flow parameters, or solution parameters. It is an intermediate step in the overall process of creating a usable model which is exported, as a mesh file, to be read in Fluent.

IV. BOUNDARY CONDITION

In the present study, velocity-inlet boundary condition was imposed on pump inlet position. It was specified to be normal to the boundary and it is defined with reference to the absolute frame. Out flow boundary condition was imposed at outlet with a flow rate weighting of 1. Outer walls were stationary but the inner walls were rotational. There were interfaces between the stationary and rotational regions. Also non-slip boundary conditions have been imposed over the impeller blades and walls, the volute casing and the inlet wall. A constant angular velocity of 2900 rpm was imposed for rotating fluid.

V. METHODOLOGY

In order to calculate the flow field in the vane and channel of the casing a commercial CFD code was used. The governing integral equations for the conservation of mass and momentum were discretized using finite volume method. Then, standard k- ϵ model was adapted for turbulence calculation, from the three known k- ϵ models (Standard k- ϵ , RNG k- ϵ and Realizable k- ϵ). The standard k- ϵ model is a semi-empirical model based on model transport equations for the turbulence kinetic energy (k) and its dissipation rate (ϵ). The model transport equation for k is derived from the exact equation, while the model transport equation for ϵ was obtained using

physical reasoning and bears little resemblance to its mathematically exact counterpart. That is rated as the most used model that combines simplicity, robustness and reasonable accuracy. Moreover, it has been tested in a wide range of industrial flows showing satisfactory results. In the derivation of the k-ε model, it is assumed that the flow is fully turbulent, and the effect of molecular viscosity are negligible. The standard k-ε turbulence model and SIMPLE algorithm applied to solve the Reynolds-Averaged Navier-Stokes (RANS) equations. Second order upwinding is considered for the discretization of momentum, k and ε terms. The simulation is steady and Moving Reference Frame (MRF) is applied to take into account the impeller-volute interaction due to convergence precision of residual 10^{-5} . For modeling of centrifugal pumps with impeller blade from 4 to 8, Gambit, a preprocessor of CFD code of commercial software Fluent has been used. In the CFD code Fluent the two-phase flow phenomenon can be modeled in several ways. The two-phase flow models used in Fluent are Euler-Euler models. These models treat the different phases as interpenetrating continua. Since the volume of a phase cannot be occupied by the other phases, the concept of phase's volume fraction is introduced. These volume fractions are assumed to be continuous functions of space and time and their sum equals to one. The conservation equations for each phase are derived to obtain a set of equations, which have a similar structure for all phases. Constitutive relations that are obtained from empirical information are used to close these equations. Three different Euler-Euler multiphase models are available in FLUENT: the volume of fluid (VOF) model, the mixture model, and the Eulerian model. For two-phase solid-liquid Eulerian-Eulerian approach with mixture multiphase model and granular options are developed. In these simulations a sand volume fraction of 10%, density of 2500 kg/m³ and a particle diameter of 111μm has been considered. In the granular option, syamlal-obrien method applied for granular viscosity.

VI. VALIDATION

In order to validate the analysis, the simulation results of flow rate at outer circumference of the six blades impeller are compared with analytical formula used to compute the volume flow rate at impeller outlet.

The volume flow rate is given by:

$$Q = 2\pi r_2 b_2 C_{2r} \quad (11)$$

Where:

r_2 is the outer radius of the impeller

b_2 is thickness of flow passage at the outer circumference.

C_{2r} is the radial component of the absolute velocity at the outer circumference of the impeller.

The outer radius and thickness of flow passage for each design flow rate are 0.092m and unit thickness, respectively. The comparison between the design flow rate used for simulation and the flow rate obtained using the analytical formula is summarized in Table 1.

TABLE 1. COMPARISON OF VOLUME FLOW RATE OBTAINED FROM SIMULATION AND ANALYTICAL FORMULA.

Design flow rate (m ³ /s)	Radial velocity at impeller outlet, C_{2r} (m/s)	Flow rate computed using analytical formula (m ³ /s)	Percentage error (%)
0.535	0.868	0.502	6.57
0.679	1.109	0.641	5.93
0.824	1.344	0.778	5.91

As can be seen from the above table, the analytical result gives a result which is accurate and the percentage error is less than 6.57%. This shows the accuracy of both the analytical result and the CFD simulation. Generally the variation of velocity and pressure obtained in this analysis are consistent with theoretical concept in pump analysis.

VII. RESULT AND DISCUSSION

The CFD analysis of the centrifugal pump with 4, 6 and 8 bladed impeller at 2900 rpm has been shown below.

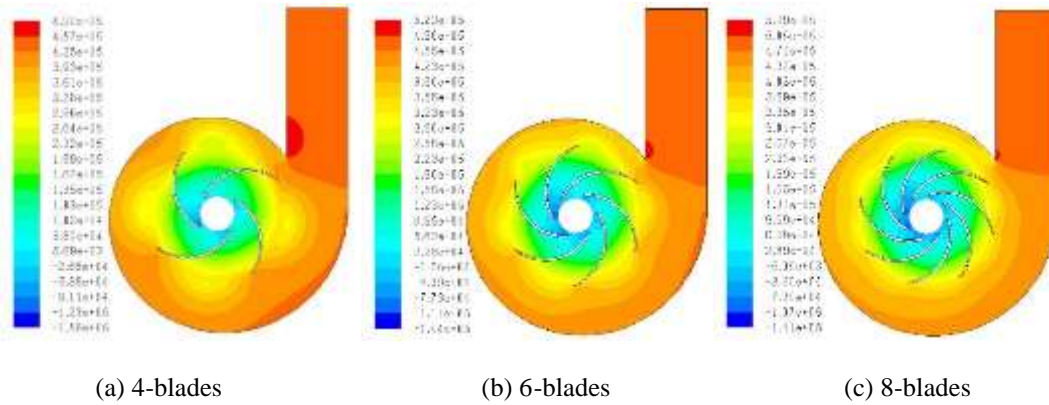


Fig. 1. Static pressure distribution of one-phase flow at the pump for different impeller

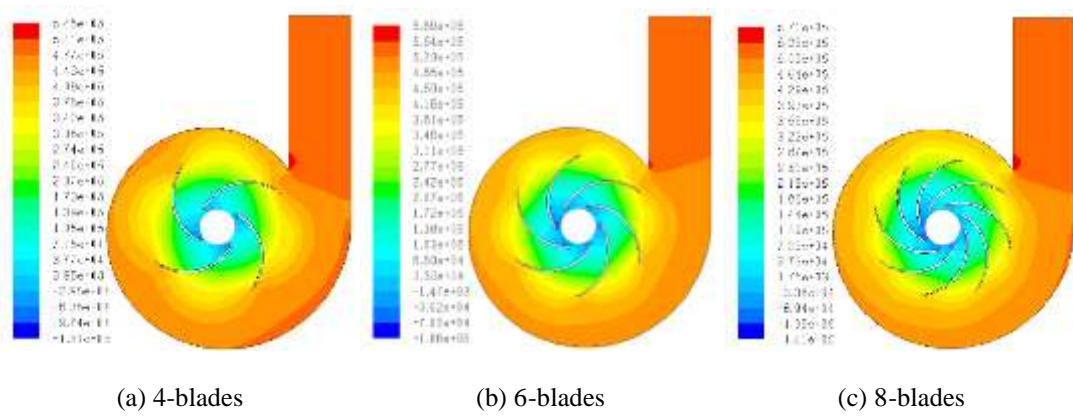


Fig. 2. Static pressure distribution of two-phase flow at the pump for different impeller

Static pressure distribution of water flow at the pump is shown in Fig. 1. From Fig. 1, it can be seen clearly that for different blade number, the static pressure gradually increase from impeller inlet to outlet, the static pressure on pressure side is evidently larger than that suction side at the same impeller radius. With the increase of the blade number, the static pressure at volute outlet grows all the time and the uniformity of the static pressure distribution at the volute become better and better. The impellers with different blade number all have an obvious low pressure area at the suction side of blade inlet, with the increase of the blade number, the area flow pressure region grows continuously, which indicates that the blade number has significant effect of pumps characteristics. Fig. 2 shows the static pressure distribution of the pump at two-phase flow. It can be seen that maximum static pressure at the pump outlet occurs in six blades number of impeller.

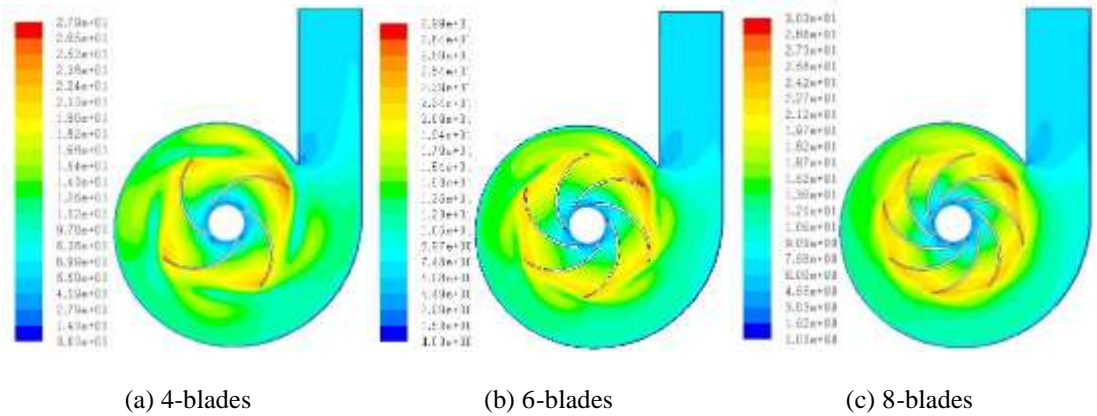


Fig. 3. Velocity contours of one-phase flow at the pump for different impeller

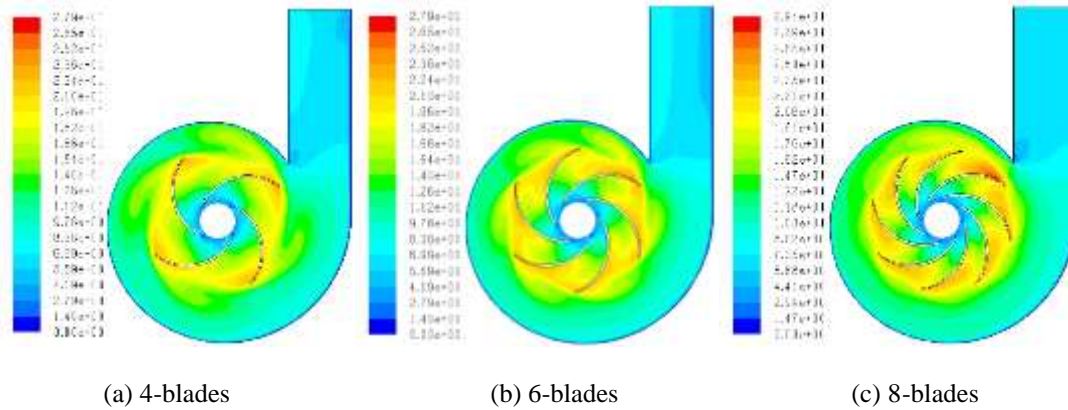


Fig. 4. Velocity contours of two-phase flow at the pump for different impeller

Study of the velocity contours gives idea about the kinetic energy and dynamic pressure acting in the different parts. Fig. 3 and 4, shows the velocity variation in the pump for different blade number of impeller, where the mechanical energy is converted into the kinetic energy. Whereas, in the casing the velocity continuously decreases as the kinetic energy is converted into fluid pressure.

Table 2: Comparison of head and static pressure of one-phase and two-phase flow through the pump

Blade number	One-phase flow		Two-phase flow	
	Static pressure at outlet (Pa)	Head (m)	Static pressure at outlet (Pa)	Head (m)
4	4.57e+05	46.67	5.11e+05	45.37
6	4.99e+05	50.96	5.54e+05	49.19
8	5.05e+05	51.57	5.36e+05	47.59

Table 2 presents the variation of head and pressure outlet of one-phase and two-phase flow. It is found from Table 2 that with increase blade number, the head of pump gradually increases. It is depicted that the pump head at the two-phase flow is smaller than the head of the water flow at the same blade number. It is also seen that the head of pump in the volute outlet is maximum in the six blades number of impeller for two-phase flow.

VIII. CONCLUSION

The flow through a centrifugal pump was analyzed using a commercial CFD package for one and two phase flow and also for different blade numbers. The simulation results are obtained at the operating speed 2900 rpm. Static pressure contours, velocity magnitude contours and head of pump at volute outlet are predicted. The mesh is generated using the Gambit part of the software. The performance results are satisfactorily matching with analytical data. The main conclusions can be summarized as follows:

- The increase of the blade number causes a growth in the static pressure and total head of the pump in the water flow.
- With the increase of the blade number, the uniformity of the static pressure distribution at the volute become better.
- The two-phase flow static pressure at the volute outlet is greater than the water flow.
- The pump head in the two-phase flow is smaller than the clear water flow.
- The pump head is maximum under the condition of having six blades at impeller.

REFERENCES

- [1] Mentzos, M., A. Filios., P. Margaris and D. Papanikas. CFD predictions of flow through a centrifugal pump impeller. Proceedings of International Conf. Experiments/Process/System Modelling/ Simulation/Optimization, 2005, Athens:1-8.
- [2] Asuaje, M., F. Bakir., S. Koudiri., F. Kenyery and R. Rey. Numerical modelization of the flow in centrifugal pump: volute influence in velocity and pressure fields. Int J Rotat, Mach 2005, 3: 244–255.

- [3] Mentzos, M., A. Filios., P. Margaritis and D. Papanikas. A numerical simulation of the impeller-volute interaction in a centrifugal pump. Proceedings of International Conference from Scientific Computing to Computational Engineering, 2004, Athens:1-7.
- [4] Boaling, C., Z. Zuchao., Z. Jianci and C. Ying. The flow simulation and experimental study of low-specific-speed high-speed complex centrifugal impellers. Chin J Chem Eng, 2006, 14(4):435-441.
- [5] Bacharoudis, E., A. Filios., M. Mentzos and D. Margaritis. Parametric Study of a Centrifugal Pump Impeller by Varying the Outlet Blade Angle. The Open Mechanical Engineering Journal, 2008, 2:75.
- [6] Caridad, J., M. Asuaje., F. Kenyery., A. Tremante and O. Aguillon. Characterization of a Centrifugal Pump Impeller under Two-Phase Flow Conditions. Journal of Petroleum Science and Engineering, 2008, 63:18.
- [7] Pagalthivarthi, K., P. Gupta., V. Tyagi and M. Ravi. CFD Predictions of Dense Slurry Flow in Centrifugal Pump Casings. International Journal of Aerospace and Mechanical Engineering, 2011, 5(4).
- [8] Anagnostopoulos, J.S. Numerical calculation of the flow in a centrifugal pump impeller using Cartesian grid. Proceedings of the Second WSEAS International Conference on Applied and Theoretical Mechanics, Venice, Italy, November 2006.